



PERGAMON

Radiation Physics and Chemistry 57 (2000) 37–51

**Radiation Physics
and
Chemistry**

www.elsevier.com/locate/radphyschem

Steady-state γ -radiolysis of aqueous methyl ethyl ketone (2-butanone) under postulated nuclear reactor accident conditions

P. Driver, G. Glowa, J.C. Wren*

AECL, Chalk River Laboratories, Fuel Safety Branch, Chalk River, Ontario, K0J 1J0, Canada

Received 25 August 1998; accepted 9 April 1999

Abstract

The steady-state γ -radiolysis of aqueous solutions containing 1×10^{-3} mol dm $^{-3}$ methyl ethyl ketone (MEK) has been studied at a dose rate of 0.12 Gy s $^{-1}$, 25°C and an initial pH of 10. Experiments were conducted in air-, Ar- or N $_2$ O-purged aqueous solutions, or in Ar-purged solutions with added *tert*-butanol. MEK, its radiolytic products, and the change in pH resulting from MEK decomposition were analysed as a function of time (or total absorbed dose). The main initial step for the radiolytic decomposition of MEK is the H abstraction from MEK by \cdot OH, produced by γ -radiolysis of water, to form MEK radical. In the absence of O, the main decay path of the MEK radical appears to be dimerization to form 3,4-dimethyl-2,5-hexanedione. In the presence of oxygen, the MEK radical reacts primarily with O to form the MEK peroxy radical. This radical ultimately results in a series of progressively smaller oxidation products. The formation of organic acids, and eventually CO $_2$, reduces the pH of the solution. This paper presents the experimental data and proposes the MEK decay kinetics and mechanism. Published by Elsevier Science Ltd.

1. Introduction

It is generally recognized that radioiodine is potentially one of the most hazardous fission products that could be released in the event of nuclear reactor accidents. This is due to the combination of its large inventory in irradiated nuclear fuel, a half-life of 8.04 d for the isotope of greatest radiological significance (131 I), a complex chemistry that may lead to the formation of volatile species, and its hazardous biological effects on the thyroid (NCRP, 1985). Thermodynamic calculations and various experiments have established

that under most accident conditions the I released from fuel into containment would be primarily in its reduced state as cesium iodide (Cubiccioiti and Sanecki, 1978; Garisto, 1982; Wren, 1983; McIsaac and Keefer, 1986). This cesium iodide would initially be dissolved in the water originating from the discharged coolant and safety spray systems. However, under highly oxidizing conditions as a result of high radiation fields following an accident, non-volatile I $^-$ initially dissolved in the containment sump water would form volatile I species (mainly I $_2$ and some organic iodides) that could become airborne (Wren et al., 1992, 1996, 1999a; Burns and Marsh, 1986; Shiraiishi et al., 1992). A breach in containment, or the need to vent the containment atmosphere to control pressure, may release a fraction of the airborne I into the environment. It is therefore important to understand the

* Corresponding author. Tel.: 613-584-3311; fax: 613-584-1220.

E-mail address: wrenc@aecl.ca (J.C. Wren)

behaviour of I in containment to predict its quantity and chemical forms (i.e. speciation) as a function of time following an accident, and to assess and minimize possible adverse effects on the environment.

These environmental concerns have prompted a great deal of study on I chemistry under conditions that would be typical of accidents (Eigen and Kustin, 1962; Boyd et al., 1980; Buxton and Sellers, 1985; Palmer and van Eldik, 1986; Buxton et al., 1988; Elliot, 1994; Lengeyel et al., 1994; Glowa, 1995; Ball et al., 1996a,b; Schwarz and Bielski, 1986; Wren et al., 1986, 1999a–c). The results of these studies have established that iodine behaviour in containment strongly depends on:

1. the steady-state concentrations of reactive water radiolysis products such as $\cdot\text{OH}$, O_2^- and H_2O_2 in the sump, as these species are involved in the oxidation of I^- (to I_2) and the reduction of I_2 (to I^-), and
2. the pH of the containment sump, because the rate of the reduction of I_2 (to I^-) is pH dependent.

These studies have also shown that under containment accident conditions, organic impurities in containment water, originating from various painted structural surfaces and other containment materials, could significantly affect the pH and the concentrations of the water radiolysis products (Spinks and Woods, 1990; Glowa, 1995; Ball et al., 1996b; Wren et al., 1999b,c). Organic iodides would also be formed thermally and radiolytically through aqueous phase reactions of I_2 with the organic impurities. The formation and decomposition of organic iodides will thus impact upon I volatility by changing the steady-state concentration of I_2 as well as by their own volatility.

Because of the impact of organic impurities on I volatility, the relative rates for the release, degradation, and formation of organic compounds and organic iodides are very important to any model describing the time-dependent behaviour of I following an accident. Thus, various studies on the effects of aqueous organic impurities on I behaviour under accident conditions have been conducted (Spinks and Woods, 1990; Glowa, 1995; Ball et al., 1996b; Wren et al., 1999b,c). These studies consisted of (a) the dissolution of organic solvents from painted surfaces into the aqueous phase, (b) the radiolysis of water containing organic impurities, originating from painted surfaces, and (c) the thermal and radiolytic decomposition and the aqueous-gas phase partitioning of organic iodides. The studies (a) and (c) above have been presented elsewhere (Wren et al., 1999b,c). A summary of the bench-scale and intermediate-scale studies on the effects of organic-painted structural surfaces on I behaviour under reactor accident conditions has also been published (Wren et al., 1999b).

The radiolytic decomposition of organic compounds in the aqueous phase has been studied in the present work using methyl ethyl ketone (MEK) to gain a detailed mechanistic understanding from which a sound strategy for modelling the effect of organic compounds on I volatility in containment following an accident can be developed. As mentioned earlier, the pH and the steady-state concentrations of water radiolysis products such as $\cdot\text{OH}$, O_2^- and H_2O_2 are important in determining the time dependent behaviour of I in containment following an accident. The effect of radiolytic decomposition of organic impurities on pH and the steady-state concentrations of water radiolysis products must be understood. MEK was chosen as a model organic compound because it is one of the common organic solvents found in paints used in containment, and because it has a relatively simple structure which allows easier quantitative analysis of the thermal and radiolytic degradation processes. The work presented in this paper is the first reported work on the detailed measurements of MEK decay and its decay products as a function of time under steady-state γ -radiolysis of aqueous solutions. Some mechanistic explanations on the dose (or time) dependence behaviour of MEK, its radiolytic decomposition products and the resulting pH change are given. We have also developed a detailed and a reduced reaction kinetic model for the radiolytic decomposition of MEK. The modelling work is presented elsewhere (Glowa et al., 1999; Wren et al., 1999d).

2. Experimental

The steady-state γ -radiolysis of aqueous solutions containing $1 \times 10^{-3} \text{ mol dm}^{-3}$ MEK was studied at a dose rate of 0.12 Gy s^{-1} , a temperature of 25°C , and an initial pH of 10 (adjusted by LiOH). The chosen concentration is of the order of the overall organic solvent level expected to be leached into the sump from painted containment surfaces in an accident. This organic level has also been observed in both bench-scale studies and the intermediate-scale studies at the Radioiodine Test Facility, as a result of organic dissolution from painted surfaces (Wren et al., 1999b).

Experiments were conducted in 25 and 50 ml glass irradiation vessels with a single neck, a stopcock and threaded top to accommodate a septum. To help ensure solution purity, irradiation vessels were rinsed with distilled, purified (Millipore Milli-Q) water, and baked at 500°C to remove organic films from the surface prior to use. Syringe needles were passed through the septum and stopcock into the main vessel for vessel purging and sample addition. To prevent the introduction of air during the removal of solution from the mixing vessel, purge gas was added to displace the

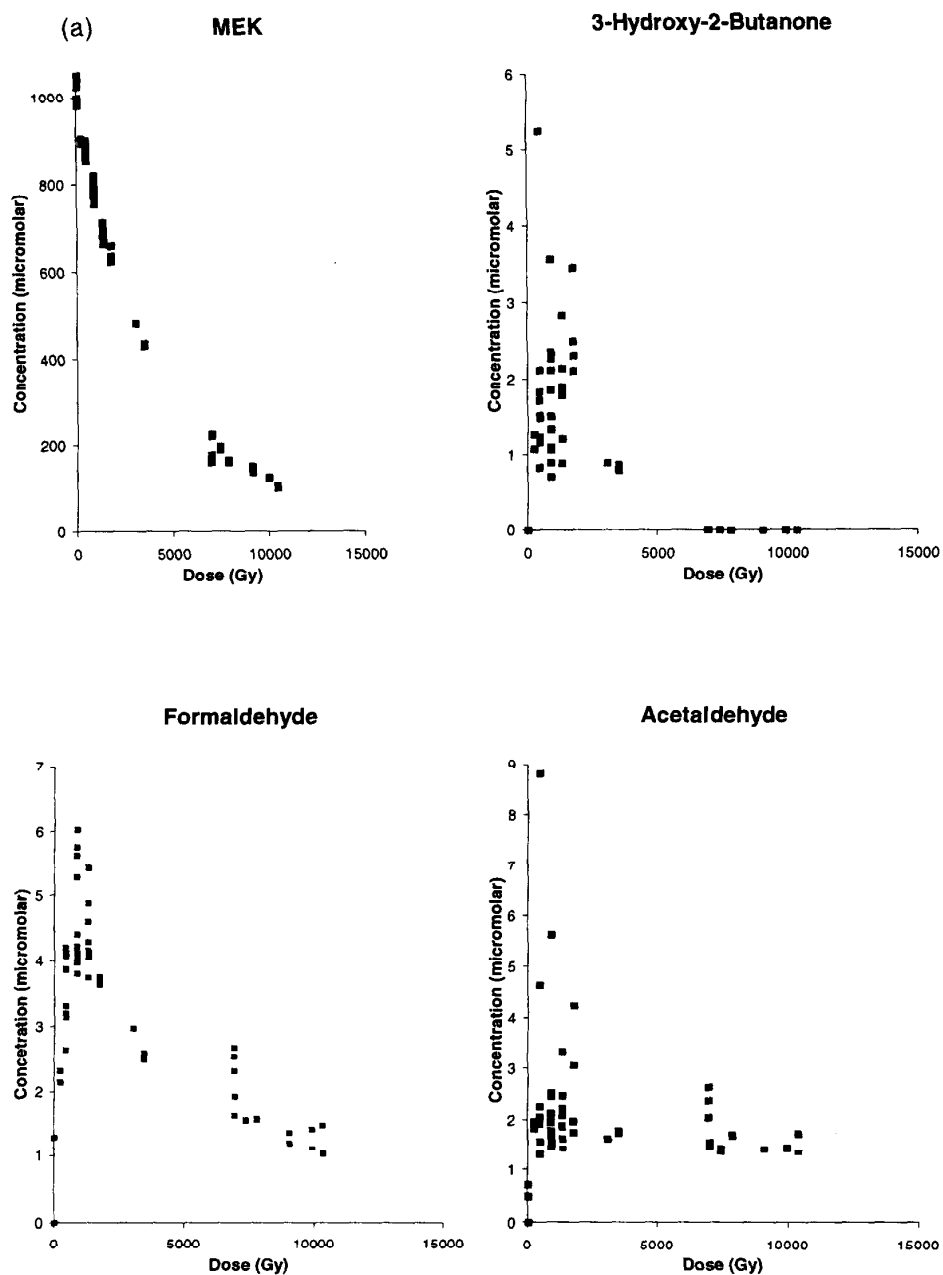


Fig. 1. (a) Product analysis for the radiolysis of Ar-purged 1×10^{-3} mol dm^{-3} MEK solutions at a dose rate of 0.12 Gy s^{-1} , a temperature of 25°C , and an initial pH of 10. (b) Product analysis for the radiolysis of Ar-purged 1×10^{-3} mol dm^{-3} MEK solutions at a dose rate of 0.12 Gy s^{-1} , a temperature of 25°C , and an initial pH of 10.

volume of the sample removed. Experiments were conducted with ultra high purity air-, Ar- or N₂O-purged aqueous solutions made with distilled, purified water (Millipore Milli-Q). The aqueous concentrations of these gases were not measured but were assumed to be saturated (i.e. 2.5×10^{-4} mol dm⁻³ O₂ or 2.5×10^{-2} mol dm⁻³ N₂O (Spinks and Woods, 1990)). To selected samples, *tert*-butanol was then added (0.5 mol dm⁻³) to modify the solution conditions. Finally, MEK was added and mixed for at least 30 min. For the aerated experiments, 50 ml vessels were filled with 5 ml liquid samples, leaving 45 ml head-space, otherwise 25 ml vessels were filled to capacity.

Samples were then irradiated in a Model 220 Gammacell ⁶⁰Co irradiator at an absorbed dose rate of ~0.12 kGy s⁻¹. Under each condition, irradiations were carried out up to ~10 kGy. Dose rates were determined by Fricke dosimetry, and subsequently corrected for ⁶⁰Co decay. All experiments were run in duplicate.

To improve detection limits, the analysis of reactant and products containing carbonyl groups was performed by high performance liquid chromatography (HPLC) on their 2,4-dinitrophenylhydrazine (DNPH) derivatives (Kieber and Mopper, 1990). Acetonitrile, and water adjusted to pH of 2.6 were passed through a 15 cm reverse phase Supelco C₁₈ model Supelcosil LC-18-DB column using a two-component gradient elution scheme. Derivatized components were detected at 370 nm. Standard solutions made up from pure compounds, and derivatized using the DNPH solution, were used to determine detector response and elution times for acetone, acetaldehyde, formaldehyde, MEK, methyl vinyl ketone, (MVK) and 3-hydroxy-2-butanone.

The analysis of organic acids was performed using a Waters 7.8 × 300 mm IC-Pak ion-exclusion column and a Waters 431 conductivity detector, using a 1 mmol dm⁻³ nitric acid isocratic mobile phase with a flow rate of 1.0 ml min⁻¹.

One of the potential MEK radiolytic products was the dimerization product of the MEK radical, 3,4-dimethyl-2,5-hexanedione. Pure 3,4-dimethyl-2,5-hexanedione was unavailable for HPLC calibration so gas chromatography coupled with mass spectrometry (GC/MS) was used to identify the MEK dimers formed in solution during irradiation. After irradiation, a 500 ml argon-purged solution of 1×10^{-3} mol dm⁻³ MEK was extracted with two 5 ml fractions of methylene chloride. The organic phase was separated and concentrated by evaporation, and 1 µl of the resulting solution analysed by GC/MS with a 25 m column (methylsiloxane). The injection port temperature was 200°C and the column temperature was initially set at 35°C. After sample injection, the column temperature was maintained at 35°C for 3 min before being ramped

to 275°C at the rate of 10°C min⁻¹. The resulting chromatogram had four peaks each of whose mass spectrum had a highest *m/e* peak at 142, the expected molecular weight of the MEK dimer. Exact mass GC/MS analysis was performed on the same sample, with the largest peak in the chromatogram giving a mass spectrum with a peak at *m/e* 142.099 ± 0.001 , which agrees with the theoretical mass *m/e* for C₈H₁₄O₂ of 142.0994.

Uncertainty in the measured concentrations is estimated to be about 5%, and higher when the concentrations were near the detection limits (ranging from ~2 µmol dm⁻³ for formaldehyde to 4 µmol dm⁻³ for MEK). However, the uncertainties in the analysis are only one component of the overall uncertainty in the data. The other components which contribute to the overall uncertainty are in the absorbed dose, variation in irradiated volume, variation in sparge gas concentration, and the presence of trace impurities. All data points have been presented to more accurately reflect overall uncertainty. The overall uncertainty in the complete irradiation procedure is impossible to estimate, but the magnitude can be seen when the scatter in individual data plots is examined.

3. Results

3.1. De-aerated solutions

3.1.1. Ar-saturated solutions

In this series of irradiations, O was removed from solution by purging with argon. This prevents O from scavenging H atoms and hydrated electrons to form relatively inert HO₂/O₂⁻ species, as well as preventing the formation of peroxy radicals.

From the radiolysis of MEK observed experimentally (Fig. 1(a)), a *G*-value of 2.8 was determined for the initial MEK loss, where the *G*-values reported in this paper are in units of the number of molecules formed or decomposed per 100 eV absorbed energy (1 molecule (100 eV)⁻¹ is equal to 0.10364 µmol J⁻¹ in SI units). The decomposition products of MEK that were observed were MEK dimers such as 3,4-dimethyl-2,5-hexanedione, and the oxidation products, 3-hydroxy-2-butanone, acetaldehyde, formaldehyde, MVK, acetone, acetic acid and formic acid. The concentration profiles of the products are shown in Figs. 1(a) and 1(b). The concentrations of these oxidation products were, however, small, about ten times lower than those found under aerated conditions (see Section 3.2). The formation of the MEK dimer was confirmed but no quantitative analysis was performed due to the difficulty in calibration without pure compound.

The radiolytic loss of MEK shown in Fig. 1(a) is replotted on a semi-log scale in Fig. 2. The concen-

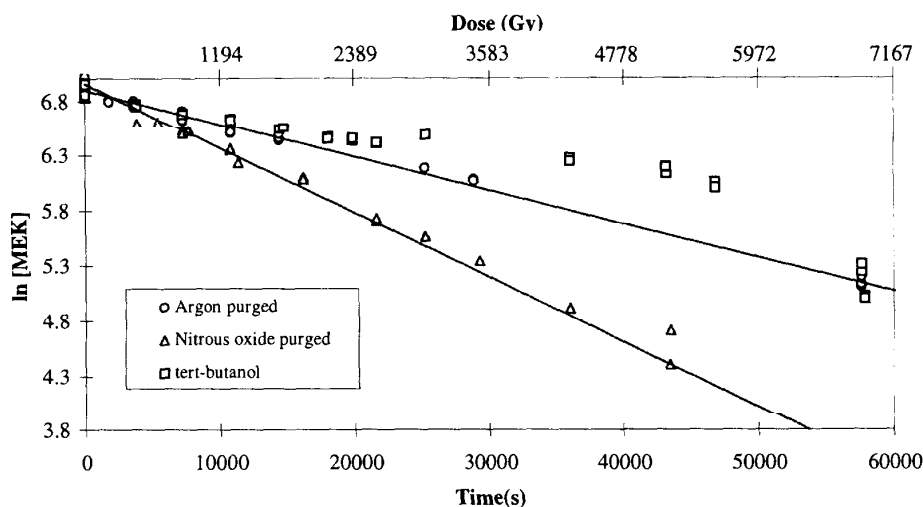


Fig. 2. The MEK decay in Ar-purged, N₂O-purged, and 0.5 M *tert*-butanol solutions is presented in a first order plot.

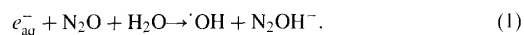
tration of MEK decreases exponentially with an increase in absorbed dose (or time at a constant dose rate), indicating that the MEK loss is a pseudo-first-order process. From the slope of the plot in Fig. 2, the pseudo-first-order rate constant for the MEK decay in Ar-purged solutions is $3 \times 10^{-5} \text{ s}^{-1}$ at a dose rate of 0.12 kGy s^{-1} .

Hydroxyl radicals or H atoms produced by γ -radiolysis of water can abstract H from MEK to form an MEK radical (Spinks and Woods, 1990). In the Ar-saturated system, the decay of the MEK radical by reaction with the residual dissolved oxygen (dissolved oxygen concentration was not measured) is very small, allowing other pathways, such as dimerization, or reactions that re-form MEK, to become prevalent. Initial evidence for the formation of MEK dimers was obtained from additional chromatogram peaks present in the carbonyl analysis of de-aerated solutions at longer retention times, which were not observed under aerated conditions. Dimerization would produce compounds such as 3,4-dimethyl-2,5-hexanedione, a species previously isolated from pure MEK after MEK radicals were produced chemically by the breakdown of diacetyl peroxide (Kharasch et al., 1948). As mentioned in the experimental section, the formation of these dimers was confirmed using GC/MS analysis on methylene chloride extractions of irradiated argon-purged MEK solutions.

3.1.2. N₂O-saturated solutions

The purpose of N₂O saturation was to isolate the effects of hydroxyl radical by converting solvated elec-

trons to hydroxyl radicals in solution by the following reaction (Spinks and Woods, 1990; Janata and Schuler, 1982):



The decrease in MEK concentration during the irradiation of a N₂O-purged aqueous MEK solution is shown in Fig. 3. A *G*-value of 5.6 was obtained for the initial MEK loss, which is approximately twice that determined for Ar-purged solutions. This value agrees well with the expected overall *G*-value for the $\cdot\text{OH}$ production in N₂O-saturated solutions (see Section 4) (Spinks and Woods, 1990; Janata and Schuler, 1982).

In the N₂O-purged solutions, the MEK concentration also decreases exponentially with increasing dose or with time at a constant dose rate (Fig. 2). The pseudo-first-order rate constant for the MEK decay at a dose rate of 0.12 kGy s^{-1} was observed to be $6 \times 10^{-5} \text{ s}^{-1}$, twice that in argon-purged solutions. This increase strongly indicates that the reaction of $\cdot\text{OH}$ with MEK is mainly responsible for the MEK loss in the Ar-purged and N₂O-saturated solutions.

The decomposition products of MEK observed in the N₂O solutions were the same as those observed in the Ar-purged solutions: 3,4-dimethyl-2,5-hexanedione, 3-hydroxy-2-butanone, acetaldehyde, formaldehyde, MVK, acetone, acetic acid and formic acid. The intermediate oxidation products were also followed as a function of dose. As expected for the case of de-aerated solutions, the levels of these oxidation products were small, only slightly higher than seen for Ar-

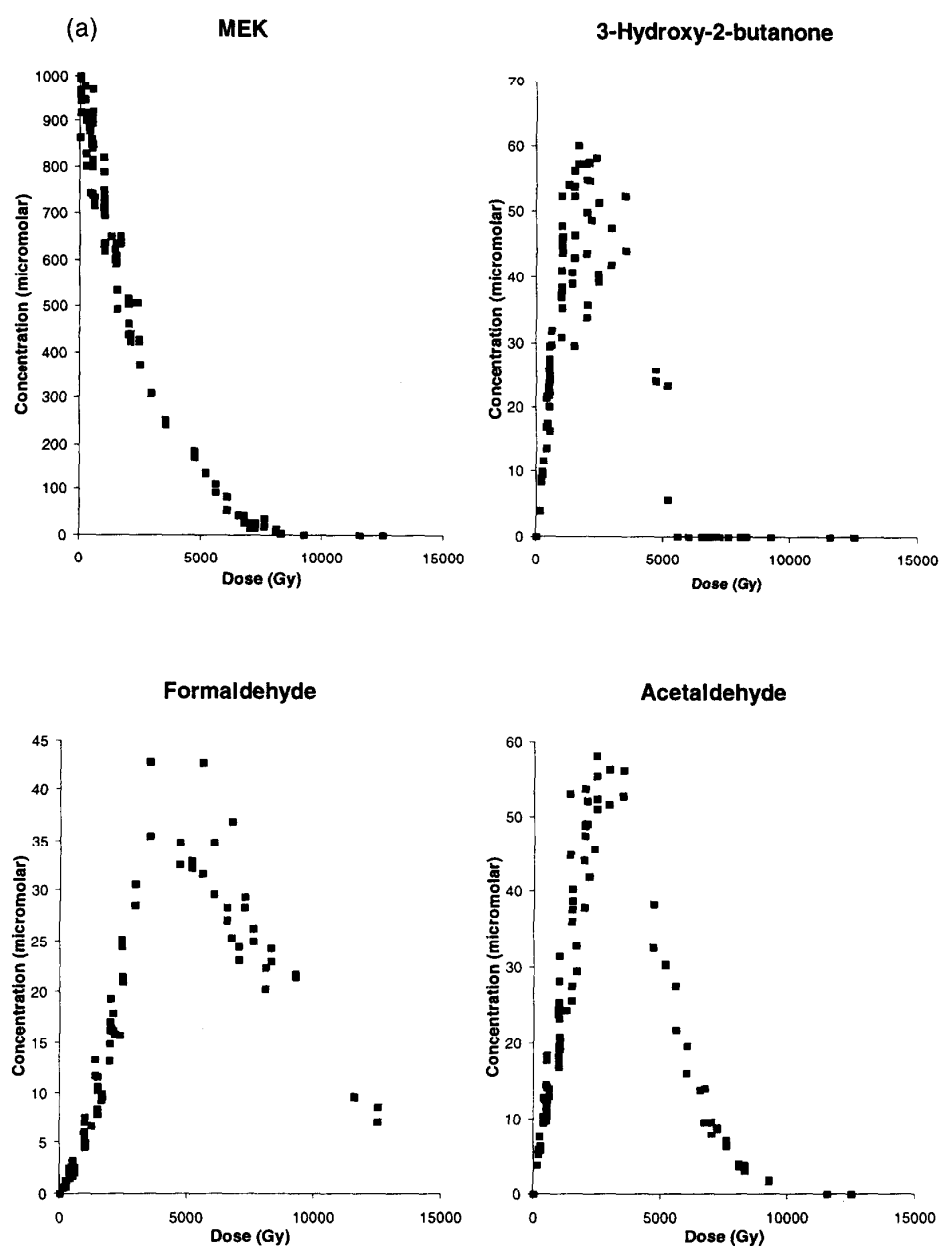


Fig. 3. (a) Product analysis for the γ -radiolysis of air-purged 1×10^{-3} mol dm $^{-3}$ MEK solutions at a dose rate of 0.12 Gy s $^{-1}$, a temperature of 25°C , and an initial pH of 10. (b) Product analysis for the γ -radiolysis of air-purged 1×10^{-3} mol dm $^{-3}$ MEK solutions at a dose rate of 0.12 Gy s $^{-1}$, a temperature of 25°C , and an initial pH of 10.

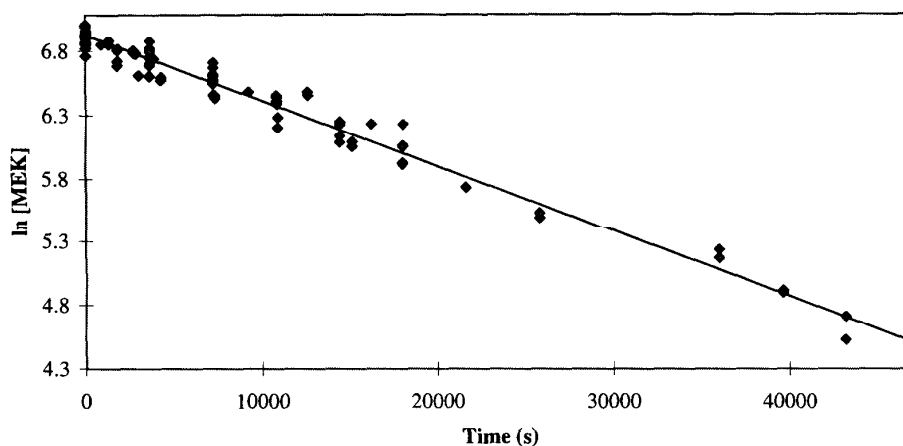


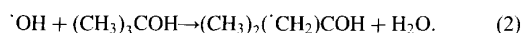
Fig. 4. The MEK decay in aerated solutions as presented in a first-order plot.

purged solutions (the results of the N_2O case are not shown because they were much the same as those obtained in the Ar-saturated case).

The major MEK radiolytic product in this case is considered to be the MEK dimers, 3,4-dimethyl-2,5-hexanedione being one of them. The higher concentration of hydroxyl radicals in solution will increase the yield of the MEK radical formed, thereby increasing the amount of the dimer formed. As expected, the size of the analogous chromatogram peaks corresponding to the MEK dimers were larger for N_2O -purged solutions than for Ar-purged solutions for the same absorbed dose. However, quantitative comparison of the MEK dimer concentrations could not be obtained in either case.

3.1.3. *tert*-Butanol solutions

The intended purpose of the addition of 0.5 mol dm^{-3} *tert*-butanol was to scavenge hydroxyl radicals (Reaction (12)), isolating the effect of solvated electrons on the radiolytic decay of MEK (Fig. 2).



Hydrogen atoms will also be scavenged, but at a lower rate (Spinks and Woods, 1990). Furthermore, since the radiochemical yield of H atoms is lower than that of hydroxyl radicals, and the rate of H abstraction from organic compounds by $\text{H}\cdot$ is much smaller than that of $\cdot\text{OH}$, only a small fraction of the MEK will decay by this pathway (see Reaction (4) vs (5) and their rate constants in Section 4). The *tert*-butanol solutions were also purged with Ar to remove O_2 .

The MEK loss was observed to have an initial G -value of 1.4, which is considerably lower than that observed for the Ar- or N_2O -purged solutions. A

simple exponential decay of MEK with time was not observed in the *tert*-butanol solutions (Fig. 2). The formation of oxidation products was also reduced to a level near or below our detection limits. A significant formation of acetone was seen, but it was determined through irradiation of reagent blanks that this occurred from the radiolytically induced decay of *tert*-butanol, not MEK. Thus, the effect of electrons is difficult to isolate experimentally. The steady-state radiolysis of MEK in the *tert*-butanol solutions is complicated by the fact that *tert*-butanol radicals are formed in solution. It is not known at this point whether these radicals react with MEK. Furthermore, the production of acetone implies the formation of small organic compounds and radicals (e.g. methyl radical) during the decomposition of *tert*-butanol. Some of these small organic radicals may have reactivity similar to that of hydroxyl radicals toward MEK. With this uncertainty in the *tert*-butanol system, the results can only be used qualitatively.

3.2. Aerated solutions

In aerated solutions, MEK degradation can proceed through reactions which involve dissolved O_2 . The concentration of MEK decreased exponentially with increasing dose (Fig. 3(a) and Fig. 4), producing a variety of oxidized products, most notably acetic acid and 2,3-butanedione. (No quantitative measurements were performed for 2,3-butanedione. The reason for this is described below. As a result, no results are presented here.) Smaller amounts of 3-hydroxy-2-butanone, acetaldehyde and formaldehyde, were also obtained, as shown in Figs. 3(a) and 3(b).

From the initial slope shown in Fig. 3(a), the G -

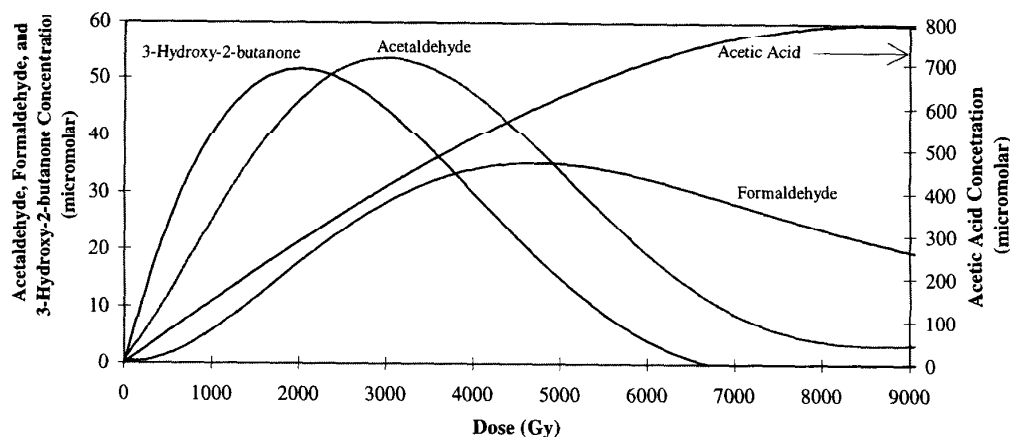


Fig. 5. Temporal profiles for intermediate products, 3-hydroxy-2-butanone, acetaldehyde, formaldehyde, and acetic acid formed during the radiolysis of aerated MEK solutions.

value for the initial loss of MEK was calculated to be 2.9. This value is again close to the primary G -value for the $\cdot\text{OH}$ production, indicating the reaction of $\cdot\text{OH}$ with MEK is mainly responsible for the MEK decay. Dissolved O scavenges the H atoms and hydrated electrons from solution leaving hydroxyl radicals to react with MEK. The O scavenged products, HO_2 and O_2^- would react with MEK but probably at slower rates than their precursors (H^\cdot or e_{aq}^-).

During the standard carbonyl compound/HPLC analysis of these irradiated solutions some samples yielded a precipitate that could not be fully dissolved in acetonitrile. This additional derivative was also found to have very low solubility in carbon tetrachloride, dimethylsulfoxide, methanol, tetrahydrofuran, hexane or methanol. By subjecting standard carbonyl compounds to this procedure, it was observed that the 2,3-butanedione derivative also displayed the same behaviour. Both species were found to dissolve sufficiently in acetonitrile to allow detection by HPLC, and showed similar highly tailed peaks. Aliquots of the 2,3-butanedione derivative and the derivative of the unknown compound were also collected, purified and analyzed by IR spectroscopy. The resemblance of the spectra supports the conclusion that the insoluble compound is the 2,3-butanedione–DNPH derivative. Due to the problem of the precipitation during the derivatization, the concentration of 2,3-butanone could not be measured quantitatively.

The formation of 2,3-butanedione and 3-hydroxy-2-butanone is followed by the formation of acetaldehyde, acetic acid, and formaldehyde with minor amounts of MVK and acetone. Acetic acid is by far the most abundant radiolytic product that was measured in this

study (Fig. 3(b)). Products such as formaldehyde were not detected initially, but were detected at higher doses. These results indicate that as the breakdown proceeds, products of progressively lower molecular weight are created in aerated systems which is opposite to the dimerization pathways noted for de-aerated solutions. It should also be noted that the DNPH analysis for carbonyls provided some smaller peaks in the HPLC chromatogram, which were not identified. The time profile of the MEK decomposition products presented in Figs. 3(a) and 3(b) are replotted in Fig. 5 to illustrate the progression of the MEK decay. When plotted on one chart in this manner, the decay profile is more easily illustrated, and provides insight into placement of each species in the decomposition mechanism. It should be noted again that although 2,3-butanedione was one of the major products identified, its time-dependent concentration profile was not obtained due to the very low solubility of the DNPH derivatized product.

Note that we have observed a small amount of MVK under aerated conditions, which is considered to be formed mainly from the MEK dimers. Thus, if only its formation is considered, a lower MVK concentration is expected in aerated solutions than in de-aerated solutions. However, the MVK concentration should be determined by its decomposition as well as its production rate. We have observed a slightly higher MVK concentration level in aerated solutions than in Ar purged solutions. Currently, we do not know its relative decomposition rates in de-aerated and aerated solutions. Furthermore, the levels of MVK that we observed both in de-aerated and aerated solutions are very low (less than twice of the uncertainty level of

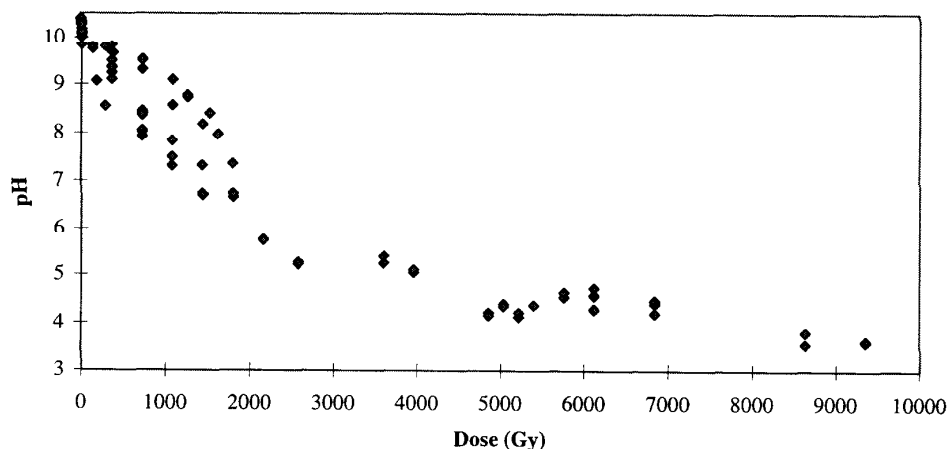


Fig. 6. pH drop during the irradiation of aerated $1 \times 10^{-3} \text{ mol dm}^{-3}$ MEK solutions at a dose rate of 0.12 Gy s^{-1} , a temperature of $25 \text{ }^\circ\text{C}$, and an initial pH of 10.

$\sim 4 \text{ } \mu\text{mol dm}^{-3}$). Its level is comparable with those of other products observed in de-aerated solutions (mostly less than $10 \text{ } \mu\text{mol dm}^{-3}$). These concentration levels are negligible, compared to the levels of oxidation products observed in aerated solutions ($50\text{--}1000 \text{ } \mu\text{mol dm}^{-3}$).

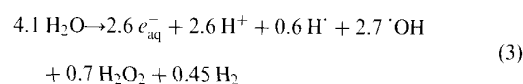
We have also measured the pH change as the result of the radiolytic decomposition of MEK in aerated solutions as a function of time (Fig. 6). The pH drop is due to the observed formation of carboxylic acids such as acetic and formic acid which, themselves, eventually decompose to CO_2 . Carbon dioxide and its associated equilibria (H_2CO_3 , HCO_3^- , CO_3^{2-}), also adds to the acidity of the solution, and can buffer the pH at the appropriate $\text{p}K_a$ s. Mass spectroscopy performed on the gas-space in the irradiation vessel confirmed that the concentration of CO_2 was increasing throughout the irradiation. The large scatter in the pH data, particularly at low doses, is considered to be due to the initial dissolved CO_2 concentration as a result of air purging and the initial pH. The buffer capacity of the carbonate system appears to have an impact on the rate of pH change (see Section 4 for further discussion).

4. Discussion

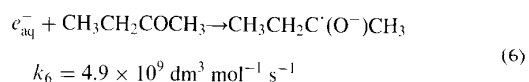
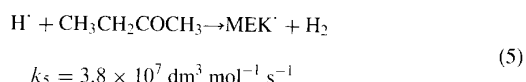
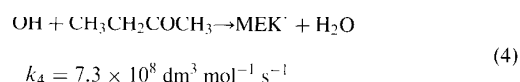
4.1. Reaction kinetics

Initial MEK decay path. In the aqueous solutions containing $1 \times 10^{-3} \text{ mol dm}^{-3}$ MEK used in this study, MEK would mainly decompose not as a result of direct absorption of γ -radiation, but through the reactions with water radiolysis products such as $\cdot\text{OH}$,

e_{aq}^- and $\text{H}\cdot$:



where the coefficients in this reaction are the G -values for the primary production of each species by γ -radiolysis of water in units of molecules produced or decomposed per 100 eV absorbed dose (Buxton et al., 1988). These water radiolysis products react with MEK (Mezyk, 1994; Mezyk and Bartels, 1994):



where MEK' represents one of the three possible hydrogen abstraction products: $\text{CH}_3(\cdot\text{CH})\text{COCH}_3$, $(\cdot\text{CH}_2)\text{CH}_2\text{COCH}_3$, and $\text{CH}_3\text{CH}_2\text{CO}(\cdot\text{CH}_2)$. The rate equation for MEK degradation is then

$$-\frac{d[\text{MEK}]}{dt} = k_4[\cdot\text{OH}] + k_5[\text{H}\cdot] + k_6[e_{\text{aq}}^-]. \quad (7)$$

Although all three reactions have potential to con-

Table 1
Initial G -value of MEK loss under various conditions

Condition	Initial G -Value of MEK loss
Argon purged, 0.5 mol dm ⁻³ <i>tert</i> -butanol	1.4
Argon purged	2.8
Aerated	2.9
N ₂ O purged	5.6

tribute to the MEK decomposition, the G -value and the pseudo-first-order rate constant for the MEK decay in N₂O-saturated solutions were observed to be twice those observed in Ar-purged solutions (Tables 1 and 2). This change in the G -value and the pseudo-first-order rate constant suggests that the reaction with $\cdot\text{OH}$ (Reaction (4)) is mainly responsible for the MEK decay and the reactions with e_{aq}^- and H^\cdot contribute very little to the MEK decay.

For continuous (or steady-state) γ -radiolysis, the concentrations of $\cdot\text{OH}$, e_{aq}^- and H^\cdot quickly reach a pseudo-steady-state with their concentrations determined by the ratio of their overall production and decomposition rates. The primary radiolysis yields (i.e. G -values) are chiefly responsible for determining the production rates of these species. Once produced, these species quickly react with each other and other water radiolysis products (Boyd et al., 1980; Buxton et al., 1988), and also other compounds present in water such as MEK and its decay products. In pure water, $\cdot\text{OH}$ reacts with many species under continuous γ -radiolysis but the key reactions are (Buxton et al., 1988):

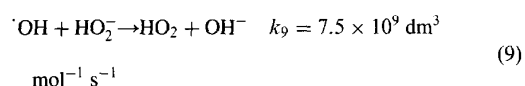
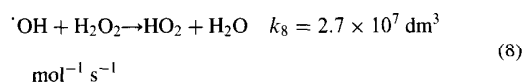
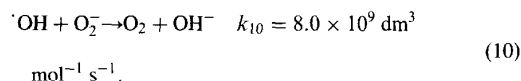


Table 2
First-order rate constant of MEK loss under various conditions

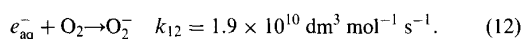
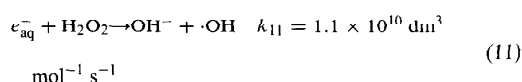
Condition	Theoretical rate (s ⁻¹)	Measured rate ^a (s ⁻¹)	R^{2b}
Argon purged	3.5×10^{-5}	$(3.1 \pm 0.1) \times 10^{-5}$	0.992
Aerated	3.5×10^{-5}	$(5.1 \pm 0.1) \times 10^{-5}$	0.978
N ₂ O purged	6.8×10^{-5}	$(5.9 \pm 0.1) \times 10^{-5}$	0.986

^a Error given is statistical error only.

^b Correlation coefficient for least squares fit.



For e_{aq}^- , the key decay reactions are:



(For a full water radiolysis model, see (Boyd et al., 1980; Buxton et al., 1988).) Note that the $\cdot\text{OH}$ production rate is determined by the primary water radiolysis yield, i.e. G -value, and the secondary reactions such as Reaction (11) has negligible impact on the production of $\cdot\text{OH}$. Using only these key decay reactions, the pseudo-steady-state concentrations of $\cdot\text{OH}$ and e_{aq}^- in pure water can be approximated as:

$$[\cdot\text{OH}]_{\text{ss}} \approx \frac{\text{const} \cdot G(\cdot\text{OH}) \cdot D_r}{k_8 \cdot [\text{H}_2\text{O}_2]_{\text{ss}} + k_9 \cdot [\text{HO}_2^-]_{\text{ss}} + k_{10} \cdot [\text{O}_2^-]_{\text{ss}}} \quad (13)$$

and

$$[e_{\text{aq}}^-]_{\text{ss}} \approx \frac{\text{const} \cdot G(e_{\text{aq}}^-) \cdot D_r}{k_{11} \cdot [\text{H}_2\text{O}_2]_{\text{ss}} + k_{12} \cdot [\text{O}_2]_{\text{ss}}} \quad (14)$$

where $G(\cdot\text{OH})$ and $G(e_{\text{aq}}^-)$ are the G -values for the primary $\cdot\text{OH}$ and e_{aq}^- production by γ -radiolysis of water, and D_r is the absorbed dose rate. The constant in this equation converts the production rate of hydroxyl radicals from molecules/100 eV (the units of G -value) to mol dm⁻³ s⁻¹.

In de-aerated solutions, the steady-state concentration of $\cdot\text{OH}$ is about two orders of magnitude higher than that of e_{aq}^- (it varies slightly with pH, dose rate and time). This is due to the fact that, although the G -values are about the same for both $\cdot\text{OH}$ and e_{aq}^- , the overall decomposition rate of $\cdot\text{OH}$ (the denominator) is about two orders of magnitude smaller than that of e_{aq}^- . For both species, the reaction with H₂O₂ is the key decomposition path and thus the ratio of k_8 to k_{11} plays a large role in determining the relative ratio of the steady-state concentrations of $\cdot\text{OH}$

and e_{aq}^- . (We have also performed calculations using a full water radiolysis model, by Boyd et al. (1980) with updated G -values by Buxton et al. (1988) for the primary water radiolysis products, which confirmed the relative ratio of $\cdot\text{OH}$ and e_{aq}^- . Sunder and Christensen (1993) found similar results.) The full water radiolysis model calculations yielded approximately three orders of magnitude lower steady-state concentration of H^\cdot than that of $\cdot\text{OH}$.

In aerated solutions, the relative ratio of the steady-state concentrations of $\cdot\text{OH}$ and e_{aq}^- is even greater due to further reaction of e_{aq}^- with O_2 . In aerated solutions, the steady-state concentration of e_{aq}^- is about three orders of magnitude lower than that of $\cdot\text{OH}$.

In the presence of MEK and its radiolysis products, the steady-state concentrations of the water radiolysis products are more difficult to calculate since the reactions of many different organic compounds must be included. It can be approximated as

$$[\cdot\text{OH}]_{\text{ss}} \approx \frac{\text{const} \cdot G(\cdot\text{OH}) \cdot D_r}{\sum_i k_i \cdot [\text{RH}_i] + k_8 \cdot [\text{H}_2\text{O}_2] + k_9 \cdot [\text{HO}_2] + k_{10} \cdot [\text{O}_2]} \quad (15)$$

and

$$[e_{\text{aq}}^-]_{\text{ss}} \approx \frac{\text{const} \cdot G(e_{\text{aq}}^-) \cdot D_r}{\sum_j k_j \cdot [\text{RH}_j] + k_{11} \cdot [\text{H}_2\text{O}_2] + k_{12} \cdot [\text{O}_2]} \quad (16)$$

where k_i (or k_j) is the rate constant of the reaction of $\cdot\text{OH}$ (or e_{aq}^-) with organic compound, RH_i (or RH_j), produced during the MEK decomposition, including MEK. The values of the first terms in the denominators are difficult to define because of the wide range of k_i (or k_j) and the concentrations of RH_i (or RH_j) at any given time. For example, the rate constant of the reaction of $\cdot\text{OH}$ with organic compounds varies widely, from $2.3 \times 10^7 \text{ dm}^3 \text{ mol}^{-1} \text{ s}^{-1}$ for acetic acid (Buxton et al., 1988), $7.3 \times 10^8 \text{ dm}^3 \text{ mol}^{-1} \text{ s}^{-1}$ for MEK (Mezyk, 1994), to $3.6 \times 10^9 \text{ dm}^3 \text{ mol}^{-1} \text{ s}^{-1}$ for acetaldehyde (Schuchmann and von Sonntag, 1988).

As predicted by the full model (Glowa et al., 1999) the steady-state concentrations of e_{aq}^- and H^\cdot are more than an order of magnitude smaller than that of $\cdot\text{OH}$, even in aqueous solution containing MEK. For example, the steady-state concentration of $\cdot\text{OH}$ during the MEK decomposition in aerated solutions is of the order of $10^{-13} \text{ mol dm}^{-3}$ (ranging from $\sim 5 \times 10^{-14}$ to $\sim 5 \times 10^{-13} \text{ mol dm}^{-3}$), whereas those of H^\cdot and e_{aq}^- are $\sim 3.5 \times 10^{-15}$ to $\sim 1.5 \times 10^{-15} \text{ mol dm}^{-3}$, respectively. These smaller concentrations of H^\cdot and e_{aq}^- ,

compared to that of $\cdot\text{OH}$ (and in the case of H^\cdot , a smaller rate constant for reaction with MEK) results in $k_4[\cdot\text{OH}] \gg k_5[\text{H}^\cdot] + k_6[e_{\text{aq}}^-]$. Therefore, the initial MEK decomposition occurs mainly through the reaction with $\cdot\text{OH}$, and the MEK reactions with H^\cdot and e_{aq}^- are concluded to be negligible.

In the *tert*-butanol solutions in which there is negligible amount of $\cdot\text{OH}$, MEK may decay through the reaction with e_{aq}^- , but the rate of this reaction should be still small since

$$-\frac{d[\text{MEK}]}{dt} \approx k_6[e_{\text{aq}}^-]. \quad (17)$$

The non-exponential decay (see discussion below), and the higher-than-anticipated rate of MEK degradation in the *tert*-butanol solutions may be a result of the reactions with the radicals produced from the degradation of the *tert*-butanol, as mentioned in the experimental section.

G -values for the initial MEK loss. We have established that under continuous γ -radiolysis, MEK decays mainly through the reaction with $\cdot\text{OH}$. This does not necessarily mean that the G -value for the initial MEK decomposition would always be the same as the G -value for the primary production of $\cdot\text{OH}$, because $\cdot\text{OH}$ can also react with other species in water as discussed above. The G -value for the MEK decomposition under the conditions of this study was observed to be the same as the G -value for $\cdot\text{OH}$ production however, suggesting that for the relatively high MEK concentration ($1 \times 10^{-3} \text{ mol dm}^{-3}$) used in this study, $\cdot\text{OH}$ reacts almost exclusively with MEK (Reaction (4)) and other $\cdot\text{OH}$ decay paths become negligible. Under these conditions, the rate equation for $\cdot\text{OH}$ becomes very simple;

$$\frac{d[\cdot\text{OH}]}{dt} = \text{const} \cdot G(\cdot\text{OH}) \cdot D_r - k_4 \cdot [\cdot\text{OH}] \cdot [\text{MEK}]. \quad (18)$$

During the initial short period when $[\text{MEK}] \approx [\text{MEK}]_0$, the $\cdot\text{OH}$ concentration is given by:

$$[\cdot\text{OH}] = \frac{\text{const} \cdot G(\cdot\text{OH}) \cdot D_r}{k_4 \cdot [\text{MEK}]_0} \quad (19)$$

where $[\text{MEK}]_0$ is the initial MEK concentration. The rate law for MEK from Reactions (13) and (17) is

$$\begin{aligned} \frac{d[\text{MEK}]}{dt} &= -k_4 \cdot [\cdot\text{OH}] \cdot [\text{MEK}]_0 \\ &= -\text{const} \cdot G(\cdot\text{OH}) \cdot D_r \end{aligned} \quad (20)$$

which can be integrated to yield

$$[\text{MEK}]_t = [\text{MEK}]_0 - \text{const} \cdot G(\cdot\text{OH}) \cdot D_r \cdot t. \quad (21)$$

Thus, the G -value for the initial loss of MEK is that

for the $\cdot\text{OH}$ production by water radiolysis, i.e. $G(\text{MEK})_0 \approx G(\cdot\text{OH})$. In nitrous-oxide saturated solutions where essentially all solvated electrons are converted to $\cdot\text{OH}$, the $G(\cdot\text{OH})$ in the equation becomes the sum of the primary $G(\cdot\text{OH})$ and $G(e_{\text{aq}}^-)$, i.e. $G(-\text{MEK})_0 \approx G(\cdot\text{OH}) + G(e_{\text{aq}}^-)$. Eq. (21) provides a simple mathematical description of MEK loss during the initial short period of irradiation which supports the experimental observations. Note that we did not assign the uncertainty on the G -value because it would vary depending upon the definition of the initial period. G -value has limited use when describing behaviour of a compound in a solution in which the decomposition or production of a compound occurs through secondary radiolytic reactions for example, reactions with $\cdot\text{OH}$ (see discussion below).

Pseudo-first-order decay kinetics. The decay of MEK was observed to follow pseudo-first-order kinetics (Fig. 4), indicating that the concentration of the main reactant, $\cdot\text{OH}$, is nearly constant with time (or at steady-state), since the rate law for MEK is

$$\frac{d[\text{MEK}]}{dt} = -k_4 \cdot [\cdot\text{OH}] \cdot [\text{MEK}]. \quad (22)$$

If the $\cdot\text{OH}$ concentration is nearly constant with time, the rate equation can be integrated to yield

$$[\text{MEK}]_t = [\text{MEK}]_0 \cdot \exp(-k_4 \cdot [\cdot\text{OH}]_{\text{ss}} \cdot t). \quad (23)$$

The concentration of MEK decreases exponentially and the slope of the plot of $\ln[\text{MEK}]$ versus time is determined by $-k_4[\cdot\text{OH}]_{\text{ss}}$.

The near constant concentration of $\cdot\text{OH}$ with time suggests that the overall average reactivity of the MEK decomposition products toward $\cdot\text{OH}$ is nearly constant with time, i.e.

$$\sum_i k_i \cdot [\text{RH}_i] \approx \text{const}. \quad (24)$$

Assuming that the average reactivity of the MEK decomposition products toward $\cdot\text{OH}$ is the same as that of MEK such that

$$\sum_i k_i \cdot [\text{RH}_i] \approx k_4 \cdot [\text{MEK}]_0 \quad (25)$$

the steady-state concentration of $\cdot\text{OH}$ would be

$$[\cdot\text{OH}]_{\text{ss}} \approx \frac{\text{const} \cdot G(\cdot\text{OH}) \cdot D_r}{\sum_i k_i \cdot [\text{RH}_i]} \approx \frac{\text{const} \cdot G(\cdot\text{OH}) \cdot D_r}{k_4 \cdot [\text{MEK}]_0}. \quad (26)$$

Using this theoretical $\cdot\text{OH}$ steady-state concentration, the slope of the plot of $\ln[\text{MEK}]$ versus time, $-k_4[\cdot\text{OH}]_{\text{ss}}$, was calculated to be $-3.5 \times 10^{-5} \text{ s}^{-1}$ for Ar-purged or air saturated solutions and 6.8×10^{-5}

 s^{-1} for N_2O saturated solutions. These theoretical values were calculated from Eqs. (23) and (26) using a $G(\cdot\text{OH})$ value of 2.7 (or 5.3 for the N_2O case) molecules per 100 eV absorbed dose, a D_r of 0.12 kGy s^{-1} , $[\text{MEK}]_0$ of $10^{-3} \text{ mol dm}^{-3}$ and a k_4 of $7.3 \times 10^8 \text{ mol}^{-1} \text{ dm}^3 \text{ s}^{-1}$ (25), which resulted in $[\cdot\text{OH}]_{\text{ss}} \approx 5 \times 10^{-14} \text{ mol dm}^{-3}$ from Eq. (26).

The pseudo-first-order plots for MEK decay observed under de-aerated conditions, shown in Fig. 2, provides rate constants of $(3.1 \pm 0.1) \times 10^{-5} \text{ s}^{-1}$ for the Ar-purged solutions, and $(5.9 \pm 0.1) \times 10^{-5} \text{ s}^{-1}$ for the N_2O -purged solutions (Table 2). These values are very close to the calculated values, 3.5×10^{-5} and $6.8 \times 10^{-5} \text{ s}^{-1}$.

The MEK decay observed in aerated solutions (Fig. 4) yielded the first-order rate constant for the MEK decay of $(5.1 \pm 0.1) \times 10^{-5} \text{ s}^{-1}$ (with a correlation coefficient of 0.978). This value is somewhat larger than the theoretical value. The difference between the theoretical and observed values is thought to be due to the simple assumption used in deriving the steady-state concentration of $\cdot\text{OH}$, that the overall rate of the reaction of MEK products with $\cdot\text{OH}$ would be the same as that of MEK. However, as mentioned earlier, the rate of $\cdot\text{OH}$ reaction with organic compounds vary widely, from $2.3 \times 10^7 \text{ dm}^3 \text{ mol}^{-1} \text{ s}^{-1}$ for acetic acid (Buxton et al., 1988), $7.3 \times 10^8 \text{ dm}^3 \text{ mol}^{-1} \text{ s}^{-1}$ for MEK (Mezyk, 1994), to 3.6×10^9 for acetaldehyde (Schuchmann and von Sonntag, 1988). The difference in the theoretical and observed first-order rate constants for the MEK decay is expected to be larger in aerated solutions than in de-aerated solutions because of the wider range and concentrations of products in the aerated solutions.

The assumption that the decay products have the same reactivity as MEK is obviously too simple. Considering the wide range of products and their reaction rates, and the simple approach in deriving both the steady-state $\cdot\text{OH}$ concentration and the rate equation for MEK, a factor of two between the experimental and theoretical values should be considered to be good.

Dose rate dependence. The steady-state concentration of $\cdot\text{OH}$ is linearly proportional to dose rate (Eq. (19) or (26)) and Eq. (23) can be expressed as a simple function of total absorbed dose ($D_T = D_r \cdot t$):

$$[\text{MEK}]_t = [\text{MEK}]_0 \cdot \exp(-\text{const} \cdot D_T). \quad (27)$$

Thus, under high MEK concentration conditions, MEK decay depends on total absorbed dose, irrespective of dose rate, although this should be confirmed by experiments performed at a different dose rate.

The linear dependence of the MEK decay rate constant on total absorbed dose applies to MEK decay only under conditions when $\cdot\text{OH}$ reacts exclusively via

Reaction (4). For low concentrations of MEK (or organic impurities), or when there are other species present, such as Γ^- , which react rapidly with $\cdot\text{OH}$, the steady-state $\cdot\text{OH}$ concentration will no longer be linearly proportional to dose rate. For example, at low concentrations (less than 1×10^{-4} mol dm $^{-3}$), the steady-state $\cdot\text{OH}$ concentration is determined not only by reaction with organic compounds but also by reactions with other water radiolysis products such as Reactions (8) and (9). Under these conditions, the rate equation for MEK is the same as those given in Eqs. (22) and (23), but the steady-state $\cdot\text{OH}$ concentration is determined by Eq. (13). The steady-state $\cdot\text{OH}$ concentration in this case no longer has a linear dependence on dose rate, because $[\text{H}_2\text{O}_2]_{\text{ss}}$ and $[\text{O}_2^-]_{\text{ss}}$ are also dose rate dependent. Under these conditions, or when other species affecting the $\cdot\text{OH}$ behaviour are present, the decomposition of MEK does not have a simple total absorbed dose dependence. The constant in Eq. (27), or kinetics based solely on G -value, thus has limited applications.

4.2. MEK decay products and mechanism

The MEK decomposition products observed in the de-aerated solutions were MEK dimer, 3,4-dimethyl-2,5-hexanedione, and various oxidation products, 3-hydroxy-2-butanone, acetaldehyde, formaldehyde, MVK, acetone, acetic acid and formic acid. The yields of the oxidation products in the de-aerated solutions are, however, about an order of magnitude lower than those in the air-saturated solutions. Small yields of oxidation products are expected in these solutions because of O produced during steady-state water radiolysis, as well as residual O remaining after purging.

The results suggest the following mechanism. The initial step in the degradation process is the removal of a H atom by $\cdot\text{OH}$ from MEK to yield a MEK radical and water. The MEK radical can then react to yield further products, or abstract a H atom from a product species with weakly bonded H to re-form MEK.

If there is no O present, the dominant MEK radical reactions are with itself to form one of the possible dimers such as 3,4-dimethyl-2,5-hexanedione (Kharasch et al., 1948).



If there is enough O present in the system, the MEK radical reacts primarily with O_2 to form MEK peroxy radical. The reaction of one of the possible MEK radicals is:

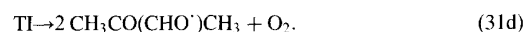
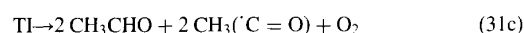


Organic peroxy radicals are known to undergo dimerization (Spinks and Woods, 1990), so the MEK peroxy

radical is considered to go through the same reaction to form a tetroxide compound:



By analogy to the acetone system studied by Zegota et al. (1986), the MEK tetroxide intermediate, TI, (MEK-O $_4$ -MEK) is considered to follow four major decay pathways:



Alkoxy radicals formed by Reaction (31d) tend to abstract a hydrogen atom from any aliphatic hydrocarbon present (Spinks and Woods, 1990). Thus, in the case of $\text{CH}_3\text{CO}(\text{CHO})\text{CH}_3$, 3-hydroxy-2-butanone will be produced. These reaction paths can explain the formation of 3-hydroxy-2-butanone, 2,3-butanedione and acetaldehyde from MEK in aerated solutions.

These intermediate MEK decomposition products are subject to similar radiolytic decay paths as MEK (i.e. abstraction of H atoms by hydroxyl radicals, followed by the reaction with dissolved O and analogous breakdown Reactions (31a) to (31d)), to form acetic acid and formaldehyde. These products are known to further decompose radiolytically to CO_2 (Spinks and Woods, 1990). This reaction mechanism explains the observed time profiles of the products showing the sequence of the MEK decomposition paths (Fig. 5).

One of the important effects on I volatility in containment following a nuclear reactor accident is the pH of the sump because it affects the reduction rate of I_2 . The suggested degradation scheme also explains the observed dose profile of pH (Fig. 6), through the evolution of acetic and formic acid, as well as CO_2 . The pH appears to be buffered initially around pH 10. Buffering may be due to the bicarbonate system, $\text{H}_2\text{CO}_3/\text{HCO}_3^-/\text{CO}_3^{2-}$ (pKa of 6.4 and 10.3, respectively) (Loewenthal and Marais, 1976), which is formed from dissolved CO_2 that is created during radiolysis under aerated conditions. Buffering in the pH 6.4 region is less obvious, because the acid concentration overwhelms the buffering capacity of the carbonate system at this point in the irradiation. The MEK decay and the pH changes as a function of dose (Figs. 3(a) and 6), suggested that at γ -radiation dose rates of 10 and 1 kGy h $^{-1}$, which are within the range of dose rate expected in containment following an accident,

90% of 1×10^{-3} mol dm $^{-3}$ MEK would be decomposed within 20 min and 4 h, respectively.

Based on the experimental results and the reaction mechanism proposed in this study, two models, a full kinetic reaction model, and a simplified model for the MEK decay in aerated aqueous solutions by γ -radiolysis have been developed. These models simulated the time dependent behaviour of the MEK decay and its decay products very well. These models and the simulation results are reported elsewhere (Glowa et al., 1999; Wren, 1999d).

5. Conclusions

The G -values observed for the initial loss of MEK under various conditions indicate that the initial step for the MEK decomposition is the abstraction of a H atom from MEK by $\cdot\text{OH}$, forming MEK radical. The MEK decay shows pseudo-first-order kinetics, indicating that the concentration of $\cdot\text{OH}$ is at steady-state during the decomposition of MEK. The MEK decay products appear to have a similar overall reaction rate with $\cdot\text{OH}$, therefore the $\cdot\text{OH}$ concentration remains constant throughout the irradiation.

The decay of MEK through the reactions with H^\cdot and e_{aq}^- was negligible because of the smaller steady-state concentrations of H^\cdot or e_{aq}^- than $\cdot\text{OH}$, particularly in the presence of O_2 , and in the case of H^\cdot also because of a lower reactivity for H abstraction from organic compounds.

In de-aerated solutions, the MEK radical mainly reacts with itself to form a dimer (3,4-dimethyl-2,5-hexanedione). In aerated solutions, the MEK radical makes use of the available dissolved O_2 to form many oxidized products such as 3-hydroxy-2-butanone, 2,3-butanedione and acetaldehyde. These intermediate products would undergo similar radiolytic decay paths as MEK, forming acetic acid and formaldehyde, which further decompose to CO_2 .

The simple first-order kinetics for the MEK decay under the steady-state γ -radiolysis conditions using the steady-state approximation for $\cdot\text{OH}$ concentration describes the observed MEK decay reasonably well. The quantitative as well as the qualitative description of the complex MEK system using the simple assumption is very important in the application of the results to nuclear safety analysis. More detailed analysis of the data has been performed using a full reaction kinetic set, whose results are reported elsewhere.

Acknowledgements

The authors would like to acknowledge Dr G.R. Burton and Dr C. Stuart at AECL and Mr K. Weaver

at Ontario Hydro for reviewing this document and for their helpful discussions. This work was funded by the COG (CANDU Owners Group) R&D Program, Working Party 06, Containment Behaviour, under the joint participation of Ontario Hydro, Hydro Quebec, New Brunswick Power and AECL.

References

- Ball, J.M., Kupferschmidt, W.C.H., Wren, J.C., 1996a. Results from phase 2 of the Radioiodine Test Facility experimental program. In: Güntay, S. (Ed.), Proceedings of the Fourth CSNI/OECD Workshop on the Chemistry of Iodine in Reactor Safety, pp. 63–81 Wurenlingen, Switzerland, NEA/CSNI/R(96)6.
- Ball, J.M., Hnatiw, J.B., Sims, H., 1996b. The reduction of I_2 by H_2O_2 in aqueous solution. In: Güntay, S. (Ed.), Proceedings of the Fourth CSNI/OECD Workshop on the Chemistry of Iodine in Reactor Safety, pp. 169–185 Wurenlingen, Switzerland, NEA/CSNI/R(96)6.
- Boyd, A.W., Carver, M.B., Dixon, R.S., 1980. Computed and experimental product concentrations in the radiolysis of water. *Radiat. Phys. Chem.* 15, 177.
- Burns, W.G., Marsh, W.R., 1986. The thermal and radiolytic oxidation of aqueous I^- and the hydrolysis and disproportionation of aqueous I_2 . United Kingdom Atomic Energy Authority, Harwell Laboratory Report, AERE R-10767.
- Buxton, G.V., Greenstock, C.L., Helman, W.P., Ross, A.B., 1988. Critical review of rate constants for reactions of hydrated electrons, hydrogen atoms and hydroxyl radicals ($\cdot\text{OH}/\cdot\text{O}^-$) in aqueous solution. *J. Phys. Chem. Ref. Data* 17, 513.
- Buxton, G.V., Sellers, R.M., 1985. Radiation induced redox reactions of iodine species in aqueous solutions. *J. Chem. Soc. Faraday Trans* 81, 449.
- Cubicciotti, D., Sanecki, J.E., 1978. Characterization of deposits on inside surfaces of LWR cladding. *J. Nucl. Mat* 78, 96.
- Eigen, M., Kustin, K., 1962. The kinetics of halogen hydrolysis. *J. Am. Chem. Soc.* 84, 1355.
- Elliot, A.J., 1994. Rate constants and G -values for the simulation of the radiolysis of light water over the range 0–300°C. Atomic Energy of Canada Limited Report, AECL 11073.
- Garisto, F., 1982. Thermodynamics of iodine, cesium and tellurium in the primary heat transport system under accident conditions. Atomic Energy of Canada Limited Report, AECL-7782.
- Glowa, G.A., 1995. Phenolic compounds as potential iodine mitigants in nuclear reactor containment. M.Sc. Thesis, University of Manitoba.
- Glowa, G.A., Driver, P.A., Wren, J.C., 1999. Irradiation of MEK Part II: a detailed kinetic model for the degradation of 2-butanone in aerated aqueous solutions under steady-state γ -radiolysis conditions. *Radiat. Phys. Chem.* (Accepted for publication).
- Janata, E., Schuler, R.H., 1982. Rate constant for scavenging e_{aq}^- in N_2O saturated solutions. *J. Phys. Chem.* 86, 2078.

- Kharasch, M.S., McBay, H.C., Urry, W.H., 1948. Reactions of atoms and free radicals in solution (XIII) reactions of diacetyl peroxide with aliphatic ketones—synthesis of 1,4-diketones. *J. Am. Chem. Soc.* 70, 1269.
- Kieber, R.J., Mopper, K., 1990. Determination of picomolar concentration of carbonyl compounds in natural waters, including seawater, by liquid chromatography. *Environ. Sci. Technol.* 24, 1477.
- Lengyel, I., Epstein, I.R., Kustin, k., 1994. Kinetics of iodine hydrolysis. *Inorg. Chem.* 32, 5880.
- Loewenthal, R.E., Marais, G.V.R., 1976. *Carbonate Chemistry of Aquatic Systems: Theory and Application*. Ann Arbor Science Publishers Inc, Ann Arbor.
- McIsaac, C.V., Keefer, D.G., 1986. Reactor building source term measurements. *ACS Symposium Series* 293, 168.
- Mezyk, S.P., 1994. Rate constant and activation energy determination for reaction of e^- and $^{\bullet}\text{OH}$ with 2-butanone and propanal. *Can. J. Chem.* 72, 1116.
- Mezyk, S.P., Bartels, D.M., 1994. Absolute rate constants measurements for the reaction of atomic hydrogen with acetone, 2-butanone, propionaldehyde and butyraldehyde in aqueous solution. *Can. J. Chem.* 72, 2516.
- National Council on Radiation Protection Measurements, 1985. Induction of thyroid cancer by ionizing radiation, NCRP No. 80.
- Palmer, D.A., van Eldik, R., 1986. Spectral characterization and kinetics of formation of hypoiodous acid in aqueous solution. *Inorg. Chem.* 25, 928.
- Schuchmann, M.N., von Sonntag, C., 1988. The rapid hydration of the acetyl radical. A pulse radiolysis study of acetaldehyde in aqueous solution. *J. Am. Chem. Soc.* 110, 5698.
- Schwarz, H.A., Bielski, B.H.J., 1986. Reactions of HO_2 and O_2^- with iodine and bromine and the I_2^- and I atom reduction potentials. *J. Phys. Chem.* 90, 1445.
- Shiraishi, H., Okuda, H., Morinaga, Y., Ishigure, K., 1992. Measurement on the rate of some reactions relevant to iodine chemistry in the aqueous phase. In: Ishigure, K., Saeki, M., Soda, K., Sigimoto, J. (Eds.), *Proceedings of the Third CSNI Workshop on Iodine Chemistry in Reactor Safety*, p. 152 Tokai-muri, Japan, 1991.
- Spinks, J.W.T., Woods, R.J., 1990. *An Introduction to Radiation Chemistry*, 3rd ed. John Wiley & Sons, Inc, New York.
- Sunder, S., Christensen, H., 1993. Gamma radiolysis of water solutions relevant to the nuclear fuel waste management program. *Nucl. Tech.* 104, 403.
- Wren, D.J., 1983. Kinetics of iodine and cesium reactions in the CANDU reactor primary heat transport system under accident conditions, Atomic Energy of Canada Limited Report, AECL-7781.
- Wren, J.C., Sagert, N.H., Sims, H.E., 1992. Modelling of iodine chemistry: The LIRIC database. In: Ishigure, K., Saeki, M., Soda, K., Sigimoto, J. (Eds.), *Proceedings of the Third CSNI Workshop on Iodine Chemistry in Reactor Safety Tokai-muri, Japan, 1991*.
- Wren, J.C., Glowa, G.A., Ball, J.M., 1986. Modelling iodine behaviour using LIRIC 3.0. In: Güntay, S. (Ed.), *Proceedings of the Fourth CSNI/OECD Workshop on the Chemistry of Iodine in Reactor Safety*, pp. 507–530 Wurenlingen, Switzerland, NEA/CSNI/R(96)6.
- Wren, J.C., Ball, J.M., Glowa, G., 1999a. The chemistry of iodine in containment, *Nucl. Tech.* (Submitted).
- Wren, J.C., Jobe, D.J., Sanipelli, G.G., 1999b. Dissolution of organic solvents from organic-based painted surfaces into water under postulated nuclear reactor accident conditions, *Can. J. Chem.* (Submitted).
- Wren, J.C., Ball, J.M., Glowa, G.A., 1999c. The interaction of iodine with organic material in containment, *Nucl. Tech.* (Accepted for publication, March).
- Wren, J.C., Glowa, G.A., Driver, P.A., 1999d. Irradiation of MEK Part III: A simplified kinetic model for the degradation of 2-butanone in aerated aqueous solutions under steady-state γ -radiolysis conditions, Manuscript in preparation.
- Zegota, H., Schuchmann, M.N., Schulz, D., von Sonntag, C., 1986. Acetylperoxy radicals, $\text{CH}_3\text{COCH}_2\text{O}_2$: A study on the γ -radiolysis and pulse radiolysis of acetone in oxygenated aqueous solutions. *Z. Naturforsch.* 41b, 1015.